Trends in Welding Research, Proceedings of the 8th International Conference
Stan A. David, Tarasankar DebRoy, John N. DuPont, Toshihiko Koseki, Herschel B. Smartt, editors, p 1-10
DOI: 10.1361/cp2008twr001

www.asminternational.org

Thermomechanical Modelling of Friction Stir Welding

J.H. Hattel, H.N.B. Schmidt and C. Tutum
Department of Mechanical Engineering
Technical University of Denmark
DK-2800 Lyngby, Denmark

Abstract

Friction Stir Welding (FSW) is a fully coupled thermomechanical process and should in general be modelled as such.
Basically, there are two major application areas of thermomechanical models in the investigation of the FSW process: i) Analysis of the thermomechanical conditions such as e.g. heat generation and local material deformation (often referred to as flow) during the welding process itself. ii) Prediction of the residual stresses that will be present in the joint structure post to welding. While the former in general will call for a fully-coupled thermomechanical procedure, however, typically on a local scale, the latter will very often be based on a semi-coupled, global procedure where the transient temperatures drive the stresses but not vice-versa.
However, in the latter, prior knowledge about the heat generation must be obtained somehow, and if experimental data are not available for the FSW process at hand, the heat generation must either be prescribed analytically or based on a fully coupled analysis of the welding process itself. Along this line, a recently proposed thermal-pseudo-mechanical model is presented in which the temperature dependent yield stress of the weld material controls the heat generation. Thereby the heat generation is still numerically predicted but the cumbersome fully coupled analysis avoided.
In the present work the formulation of all three mentioned modelling approaches as well as the very fundamental pure thermal models are briefly presented and discussed together with selected modelling results including prediction of material flow during welding, prediction of heat generation with the thermal-pseudo mechanical model as well as residual stress and deformation analysis combined with in-service loads.

Introduction

During the last decade an increasing amount of contributions have been given in literature in the field of thermomechanical modelling of FSW. These models are generally chategorized by either their area of application, i.e. flow models or residual stress models, or by the continuum mechanics approach they are based upon, i.e. Computational Solid Mechanics (CSM) models or Computational Fluid Dynamics (CFD) models, where the former typically are Lagrangian and the latter Eulerian, see figure 1.

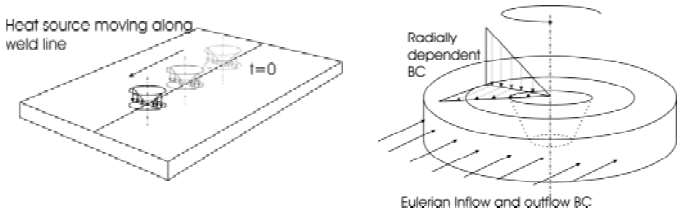

Figure 1: Left: Lagrangian model of FSW. Right: Eulerian model of FSW, [1].

The equations for conservation of momentum, energy and mass, respectively are in the Lagrangian and Eulerian frames given by

Table 1: Governing equations for conservation of momentum, energy and mass, respectively in Lagrangian and Eulerian frames.

Lagrangian frame Typically CSM	**Eulerian frame** Typically CFD
Energy	
$\rho c_p \dot{T} = \left(kT_{,i}\right)_{,i} + \eta s_{ij} \dot{\varepsilon}_{ij}^{pl}$	$\rho c_p \dot{T} = \left(kT_{,i}\right)_{,i} + \eta s_{ij} \dot{\varepsilon}_{ij}^{pl} - u_i (\rho c_p T)_{,i}$
Momentum	
$\rho \ddot{u}_i = \sigma_{ji,j} + p_i$	$\partial\left(\rho \dot{u}_i\right)/\partial t = \sigma_{ji,j} + p_i - \rho(\dot{u}_j \dot{u}_i)_{,j}$
Mass	
No explicit equation	$\dot{\rho} = -(\rho u_i)_{,i}$

These are the fundamental, governing partial differential equations that depending on the continuum mechanical framework that is used will need to be modified and combined with proper constitutive laws for the particular case at hand. In the following, the basis of thermal models, computational solid mechanics (CSM) models, computational fluid dynamics (CFD) models and the new thermal-pseudo-

mechanical model for FSW are shortly presented and the above shown equations are modified accordingly. It should be mentioned that although microstructural models and their coupling to mechanical properites are very important for predicting the behaviour of FSW welds, they are not discussed in the present work.

Thermal models

Thermal modelling has since the late nineties been a central part of modelling of FSW in general (some major contributions are given in [2-10]). One of the reasons for this is that many of the properties of the final weld are directly a function of the thermal history which the workpiece has been exposed to. Secondly, the FSW process itself is highly affected by the heat generation and heat flow and thirdly, from a modelling viewpoint, thermal modelling of FSW can be considered the basis of all other models of the process, be it microstructural, CFD or CSM models. In the FSW process the welding parameters are all chosen such that the softening of the workpiece material enables the mechanical deformation and material flow. However, unlike many other thermomechanical processes, the mechanisms of FSW are fully coupled meaning that the heat generation is related to material flow and frictional/contact conditions and vice versa. Thus, in theory a thermal model alone cannot predict the temperature distribution/history without a pre-knowledge about the heat generation, since the fundamental mechanisms of FSW are not part of a pure thermal model. For this reason, several analytical expressions have been given in literature for the heat generation for a given weld as a function of tool geometry and welding parameters, e.g. tool radius and rotational speed. This means that in the energy equation in table 1, the plastic dissipation term is replaced by a heat source term, see table 2, line 1.

Table 2: Governing equations for conservation of energy in thermal models, respectively in Lagrangian and Eulerian frames

Lagrangian frame	**Eulerian frame**
Energy with source term	
$\rho c_p \dot{T} = \left(kT_{,i}\right)_{,i} + \dot{Q}'''$	$0 = \left(kT_{,i}\right)_{,i} + \dot{Q}''' - u_i \left(\rho c_p T\right)_{,i}$
Energy without source term but all heat prescribed at surface	
$\rho c_p \dot{T} = \left(kT_{,i}\right)_{,i}$	$0 = \left(kT_{,i}\right)_{,i} - u_i \left(\rho c_p T\right)_{,i}$

In all thermal models of FSW the main task now is to solve this energy equation with an appropriate set of initial and boundary conditions. However, in most pure thermal models of FSW, the heat generation from both frictional and plastic dissipation is modelled via a surface flux boundary condition at the tool/matrix interface, see table2, line 2.
The main unknown parameters in these surface flux expressions are either the friction coefficient under the assumption of sliding and the material yield shear stress under the assumption of sticking.

Along this line, the authors have proposed the following generally adopted equation for the total heat generation, [7], (see figure 1)

$$\begin{aligned} Q_{total} &= \delta Q_{sticking} + (1-\delta) Q_{sliding} \\ &= \frac{2}{3}\pi\omega\left[\delta\tau_{yield} + (1-\delta)\mu p\right]\times \\ &\left[\left(R^3_{shoulder} - R^3_{probe}\right)(1-\tan\alpha) + R^3_{probe} + 3R^2_{probe}H\right] \end{aligned} \quad (1)$$

Where δ is the dimensionless slip rate between the tool and the work piece (1 for full sticking and 0 for full sliding).

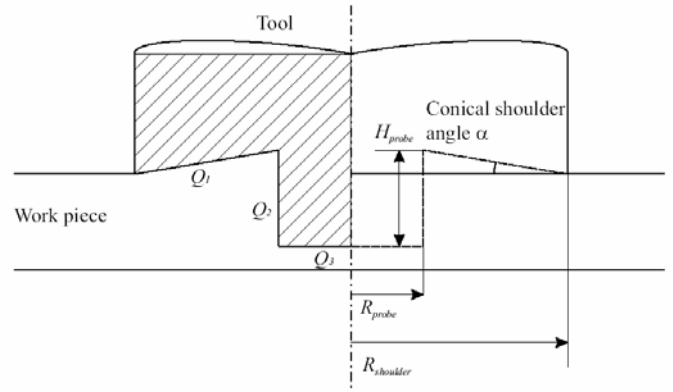

Figure 2: Different contributions from the shoulder and the pin to the surface heat generation, [6].

However, when implementing this into a numerical model using a position dependent surface flux [Wm^{-2}], it is typically used on the following form, [6],

$$\begin{aligned} q_{total} &= \dot{\gamma}\tau_{friction} + (\omega r - \dot{\gamma})\tau_{yield} \\ &= \omega r\left[\delta\tau_{yield} + (1-\delta)\mu p\right] \end{aligned} \quad (2)$$

which in fact is the basis for deriving equation (1). Furthermore, when combining equation (1) and (2) and assuming the simple tool geometry of a flat shoulder only, one obtains the following well-known expression for the heat generation [Wm^{-2}], see e.g. [7],

$$q_{total} = \frac{3Q_{total}r}{2\pi R^3_{shoulder}} \quad (3)$$

which can be applied as a radius dependent surface flux in the model, under the assumption of a constant contact condition close to sliding or in cases of sticking where the shear layer is very thin.

From equation (3) it can be seen that Q_{total} can be considered an input parameter in the same manner as the friction coefficient, the pressure and the material's yield shear stress in equation (1). However, it should be mentioned that having Q_{total} as part of the input parameters for the model in some

situations could conflict with the very objective for thermal modelling of FSW. This is especially the case when the model should predict temperatures for conditions not supported by measurements of the heat input Q_{total}. In these cases it is not straightforward to predict or simulate the effect of e.g. a change in welding or rotational speed, because the total heat generation Q_{total} is a function of these changes in parameters and hence can be considered an internal function of the FSW process; unlike other welding process, e.g. TIG where the heat input is controlled externally.
This dilemma can of course be overcome by supporting the thermal model with a thermo-mechanical CSM or CFD based model which "includes" the underlying physics of the process, namely the material flow producing heat generation by plastic dissipation in the shear layer and frictional contact at the tool/workpiece. As being pretty obvious from the later sections on CSM and CFD models, the efforts for such simulations are highly demanding from both a computational and a human resource point of view, thus leaving pure thermal modelling of FSW as a valuable "simple" alternative for simulation of heat flow having in mind the limitation of such models, which as earlier mentioned primarily lie in the evaluation of Q_{total}.
Having said that, it should be noted that the most utilized procedure for evaluating Q_{total} typically is to rely on experimental findings by simply performing the actual welds and measuring Q_{total} with a dynamometer, and thereby accepting the inherent limitation of the resulting thermal model to predicting only temperatures for a *known* total heat generation.

Since the prescribing of the heat generation is the most single important parameter in thermal models of FSW the authors proposed a classification of different heat sources [7].
One characteristic in this classification is how "detailed" the tool heat generation is resolved. Three levels were evaluated, i.e. i) including shoulder heat generation, without probe heat generation, ii) including shoulder and probe heat generation, with probe material and iii) shoulder and probe heat generation but without probe material.
A second characteristic was whether the convective contribution due to the material flow in the shear layer was taken into account. Two extreme contact conditions were evaluated, i.e. full sliding and full sticking. In the case of sliding the heat was applied as a surface flux and in the case of sticking the heat was applied as a volume flux in a shear layer. This shear layer was prescribed analytically assuming a uniform thickness with a linear velocity profile ramped between the tool velocity at the contact interface and the welding velocity outside the shear layer.
It was concluded that for analysing the temperature field in the volume under the tool, special attention should be paid to how the heat generation and the material "flows" around the tool probe. The main effect of including the probe in the thermal model is to change the material properties to those of the tool; secondly, rotating the probe and modelling the shear layer around it such that it resembles a flow model.

One new procedure to obtain the heat generation is to couple the traditional analytical expression for the heat generation with a constraint based on experimental or phenomenological considerations. It is well-known from the constitutive behaviour of a solid (representative for those alloys used in FSW), that the yield stress dramatically decreases once the temperature approaches the solidus temperature. Above the solidus temperature, the material acts as a fluid. As a consequence, the material close to the tool/matrix interface will reduce its heat generation to negligible values if exceeding the solidus temperature – reducing the temperature level – allowing the material to recover its strength. A self-stabilizing effect will thus establish at a temperature level around the solidus temperature, hence this could be used as an average temperature constraint in a pure thermal model. This is what is done in the thermal model by Tutum *et al*. [10] where the heat generation in FSW of AA2024 is controlled by using an optimization scheme such that an *average* temperature of 500 ^{o}C at the tool/workpiece interface is obtained.
This procedure has given promising results for obtaining temperature fields without prior knowledge regarding Q_{total} – in fact this is an output of the optimization analysis.

Computational Solid Mechanics Models

As mentioned before, the two reasons for doing solid mechanics models of FSW are to predict the flow and to predict the residual stresses. The main governing equations for these types of models are given in table 3. The energy equation will essentially be as shown in table 1, line 1 (giving a fully coupled thermomechanical model) or table 2 (giving a sequentially coupled thermomechanical model) depending on the choice of thermal model. For the solid mechanically based *flow modelling* there are basically two approaches: The simplest is to assume a rigid-visco-plastic material, i.e. the total strain is equal to the visco-plastic strain and use an implicit solver based on quasi-static equilibrium. This is done by several authors in literature, see e.g. [12-14].
The more comprehensive approach is to use the dynamic equilibrium equation and to take all the contributions to the strain into account although the viscoplastic part obviously is the dominating contribution. This is typically done in an ALE formulation where the dynamic equilibrium equation is solved in an explicit manner. This approach has been used by several authors, see e.g. [15-18]. A special feature about the model by Schmidt and Hattel [17] (implemented in ABAQUS Explicit) is that the heat generation between the tool and the matrix is not prescribed but part of the solution itself. This adds to the generality of the model but also to the complexity and hence the need for computational power.
The model [17] has been used to predict among others the plastic strain in the weld which resembles the well-known "flow arm" quite well, see figures 3 and 4 as well as the void

formation behind the tool, see figure 6, being the first model in literature able to predict this.

Table 3: Basic equations for solid mechanics models of FSW for flow and residual stresses, respectively

Flow during welding	**Residual stresses**
Momentum	
Dynamic equilibrium, e.g. explicit ALE $\rho\ddot{u}_i = \sigma_{ji,j} + p_i$	Dynamic equilibrium not relevant
Static equilibrium, e.g. implicit "flow formulation" $\sigma_{ji,j} + p_i = 0$	Static equilibrium. Quasi-static thermomechanical analysis $\sigma_{ji,j} + p_i = 0$
Strain vs. displacements	
Large strain theory $\varepsilon_{ij}^{tot} = \frac{1}{2}(u_{i,j} + u_{j,i} + u_{k,i}u_{k,j})$	Small strain theory $\varepsilon_{ij}^{tot} = \frac{1}{2}(u_{i,j} + u_{j,i})$
Total strain	
Rigid viscoplastic: $\varepsilon_{ij}^{tot} = \varepsilon_{ij}^{vp}$ Explicit ALE $\varepsilon_{ij}^{tot} = \varepsilon_{ij}^{el} + \varepsilon_{ij}^{pl} + \varepsilon_{ij}^{vp} + \varepsilon_{ij}^{th}$	Rate independent plasticity $\varepsilon_{ij}^{tot} = \varepsilon_{ij}^{el} + \varepsilon_{ij}^{pl} + \varepsilon_{ij}^{th}$
Thermal strain	
$\varepsilon_{ij}^{th} = \delta_{ij}\int_{T_1}^{T_2}\alpha(T)dT$	
Constitutive law	
Equivalent stress $\bar{\sigma} = \left(\frac{3}{2}\sigma_{ij}\sigma_{ij}\right)^{1/2}$ Equivalent total strain rate (rigid viscoplastic) $\dot{\bar{\varepsilon}}^{tot} = \left(\frac{2}{3}\dot{\varepsilon}_{ij}^{tot}\dot{\varepsilon}_{ij}^{tot}\right)^{1/2}$ Yield stress, in general: $\sigma_y = \sigma_y(T, \dot{\bar{\varepsilon}}^{pl})$ $\sigma_y \to 0 \quad T \to T_{cut-off} \sim T_{sol}$ Norton power law $\sigma_y = K\dot{\bar{\varepsilon}}^m$ Inverse hyperbolic sine $\sigma_y = \frac{1}{\alpha}\sinh^{-1}\left(\frac{Z}{A}\right)^{1/n}$ $Z = \dot{\bar{\varepsilon}}e^{Q/RT} \qquad m = \frac{\partial \ln \bar{\sigma}}{\partial \ln \bar{\varepsilon}}$ Johnson-Cook $\sigma_y = \left(A + B\bar{\varepsilon}^n\right)\left(1 + C\ln\frac{\dot{\bar{\varepsilon}}}{\dot{\varepsilon}_0}\right) \times\left(1 - \left(\frac{T - T_{ref}}{T_{sol} - T_{ref}}\right)^m\right)$	Equivalent stress $\bar{\sigma} = \left(\frac{3}{2}\sigma_{ij}\sigma_{ij}\right)^{1/2}$ Equivalent plastic strain $\bar{\varepsilon}^{pl} = \left(\frac{2}{3}\varepsilon_{ij}^{pl}\varepsilon_{ij}^{pl}\right)^{1/2}$ Yield stress, in general: $\sigma_y = \sigma_y(T, \bar{\varepsilon}^{pl})$ $\sigma_y \to 0 \quad T \to T_{cut-off} \sim T_{sol}$ Hardening law, e.g. Ramberg-Osgood: $\bar{\varepsilon}^{tot} = \frac{\sigma}{E} + \alpha\frac{\sigma_y}{E}\left(\frac{\sigma}{\sigma_y}\right)^n$ Elasticity Hooke's generalized law $\sigma_{ij} = \frac{E}{1+\nu}\left(\varepsilon_{ij}^{el} + \frac{\nu}{1-\nu}\delta_{ij}\varepsilon_{ij}^{el}\right)$

Apart from modelling the flow, the purpose of the computational solid mechanics models of FSW obviously is to find residual stresses, see e.g. [19-22]. As seen from table 3 it is clear that these ressidual stress models typically are based on a thermo-elasto-plastic description, whereas the flow models are based on rigid-visco-plastic models in most cases.

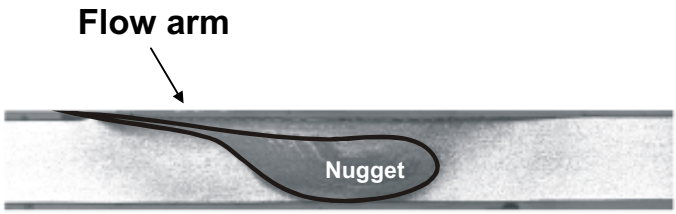

Figure 3: Micrsotructure showing the well-known "flow arm" from the nugget, [17].

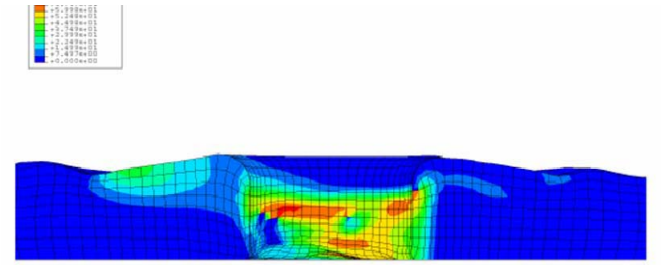

Figure 4: Numerically predicted equivalent plastic strain (in the range of 0-75) showing a similar result in figure 4, [17].

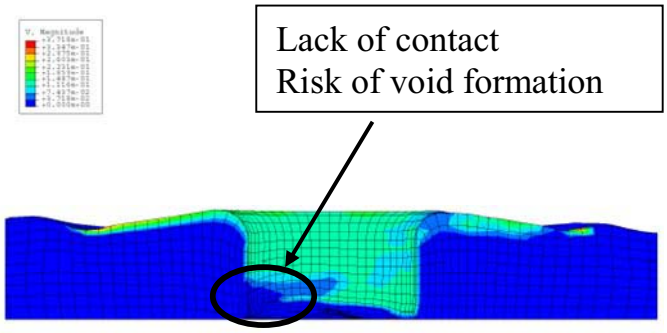

Figure 5: Numerically predicted size of velocity. Note the lack of contact resulting in risk of void formation at the advancing side, [17].

An analysis of the residual stresses and the coupling to the subsequent load situation was carried out by the authors in ABAQUS Standard on a structure where a stringer is friction stir welded onto a plate [22], see figure 6.
The integrated residual stress and load analysis consisted of four steps which are shown in figure 7.
The residual stresses along the dotted line shown in figure 7 after welding and releasing as well as after applying the load are presented in figure 8.
As seen on the figure, applying the load actually slightly reduces the longitudinal stresses in the middlle of the weld. This is of course not a general statement but only valid for this

geometry and load case. Moreover, it should be emphasized, that this type of analysis obviously would benefit a lot from a prediction of the transient evolution of the mechanical properties in the structure close to the weld.

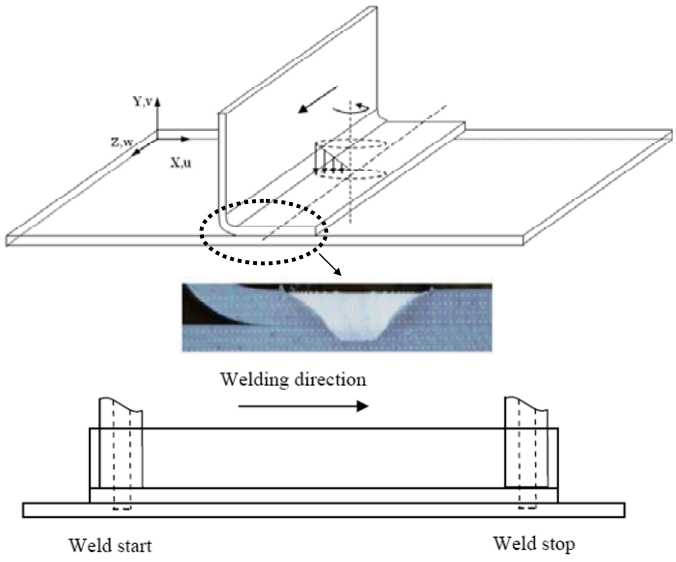

Figure 6: Geometry of a stringer friction stir welded to a plate. Used for coupling of residual stress and in-service load analyses, [22].

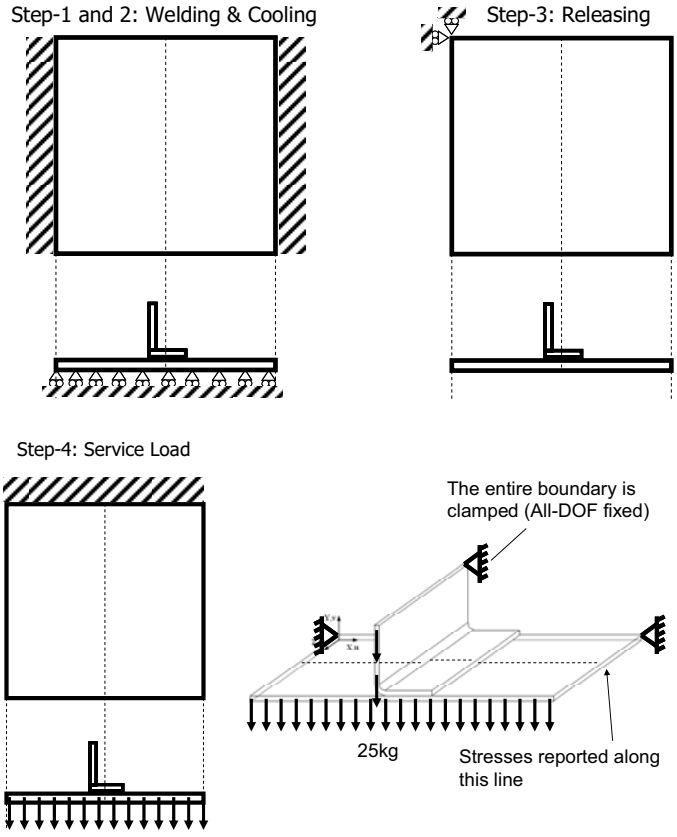

Figure 7: The 4 steps in the coupled residual stress and in-service load analyses, [22]

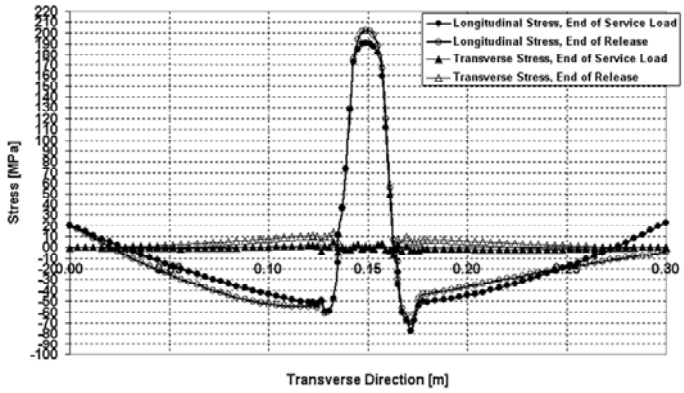

Figure 8: Longitudinal and transverse residual stresses after welding and releasing as well as after applying the load, [22].

Computational Fluid Dynamics Models

Traditionally speaking, CFD models will not be considered as being of "thermomechanical type" in computational welding mechanics. In conventional welding processes, CFD models are normally used for weld pool dynamics and CSM models for residual stresses. However, in FSW both CSM models as the ABAQUS Explicit model mentioned above [17] and CFD models as the one that will be shown in the following can be used to find the material flow during welding. For this reason it makes good sense to present the CFD approach to material flow in FSW, anyway.

The basic assumption in the CFD models obviously is to treat the matrix material as a fluid, see table 4 for an overview of the governing equations. In particular, this calls for a suitable constitutive model from which the viscosity can be expressed. In literature, it is the most common for FSW to use the inverse hyperbolic sine law, see tables 3 and 4, for the yield stress as a function of the shear rate. This expression captures both the power law regime for low strain rates and the power law breakdown at higher strain rates. CFD models are typically formulated in a Eulerian frame, so that the tool is stationary, hence only rotating and the welding speed is accounted for by having incoming and outgoing material flow at the boundaries. The energy equation will be that of table 1, line 1 (right) for a fully-coupled model or table 2, lines 1 and 2 (right) for a sequentially coupled model.

Some important contributions to flow modelling in FSW based on CFD can be found in [23-27].

In Figures 9 and 10, a comparison between experiment, analytically based streamlines and a CFD model (implemented in COMSOL) is shown, [28]. The experiment contained of welding through a line of Cu marker material (MM) in two plates of 2024 and then unscrewing the tool as its center was aligned with the line of MM.

Based on experimental findings in terms of CT pictures and comparisons with theoretical predictions by both analytical and numerical flow models, the authors, [28], have proposed

three characteristic zones for the flow around the tool probe: i) the rotation zone. ii) the transition zone and iii) the deflection zone, see Figure 11. It should be mentioned that this classification is based on a simplified representation of the real, more complex flow – thus not taking into account 3D flow effects, non-symmetrical tool features (e.g. threads) and cyclic contact condition (collapse of the shear layer).

Table 4: Basic equations for fluid mechanics models of FSW for flow

Momentum	
Steady state $0 = \sigma_{ji,j} + p_i - \rho(\dot{u}_j \dot{u}_i)_{,j}$	Steady state, Stokes flow $0 = \sigma_{ji,j} + p_i$
Strain rates vs. displacement rates	
$\dot{\varepsilon}_{ij}^{Tot} = \frac{1}{2}(\dot{u}_{i,j} + \dot{u}_{j,i})$	
Constitutive law	
Incompressible Newtonian $\sigma_{ij} = -\delta_{ij} P + 2\mu\dot{\varepsilon}_{ij}$ Eq. stress vs. eq. strain rate $\bar{\sigma} = K\dot{\bar{\varepsilon}} \quad (m=1)$ Cut-off temperature $\mu \to 0 \quad T \to T_{cut-off} \sim T_{sol}$	Incompressible non-Newtonian $\sigma_{ij} = -\delta_{ij} P + \mu_{eff} 2\dot{\varepsilon}_{ij}$ Eq. stress vs. eq. strain rate $\bar{\sigma} = K\dot{\bar{\varepsilon}}^m$ Effective viscosity, in general $\mu_{eff} = \frac{\bar{\sigma}}{3\dot{\bar{\varepsilon}}} \Rightarrow \mu_{eff} = \mu\sqrt{3}^{m-1}\dot{\bar{\varepsilon}}^{m-1}$ Effective viscosity, power law $\mu_{eff} = \frac{1}{3}K\dot{\bar{\varepsilon}}^{m-1}$ Effective viscosity, inv.hyp.sine $\mu_{eff} = \frac{\frac{1}{\alpha}\sinh^{-1}\left\{\frac{1}{A}\dot{\bar{\varepsilon}}e^{-Q/RT}\right\}^{1/n}}{3\dot{\bar{\varepsilon}}}$ Cut-off temperature $\mu_{eff} \to 0 \quad T \to T_{cut-off} \sim T_{sol}$

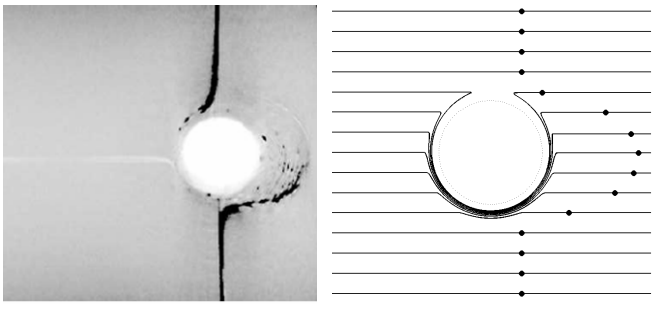

Figure 9: Left: CT picture of weld with transverse MM. Exit hole aligned with the MM plane. Right: Analytically obtained stream lines/tracer particles, [28].

The CFD models are very suitable for analyzing the material flow during FSW, however they have some important limitations that should be mentioned: i) The residual stresses after welding which are of great importance cannot be captured, since a CFD model in nature is rate dependent only. ii) The elastic stress state in the area "far away" from the tool is not properly described. iii) The contact condition at the tool/interface is typically not very well described in the present CFD models of FSW, i.e. an a priori prescribed velocity emulating either sticking or sticking/sliding is normally used. These three limitations mentioned for the CFD models are all more or less eliminated if the material flow is described by computational solid mechanics models. These, on the other hand, often have the disadvantage of high demands for remeshing, which the CFD models, being of Eulerian nature, do not.

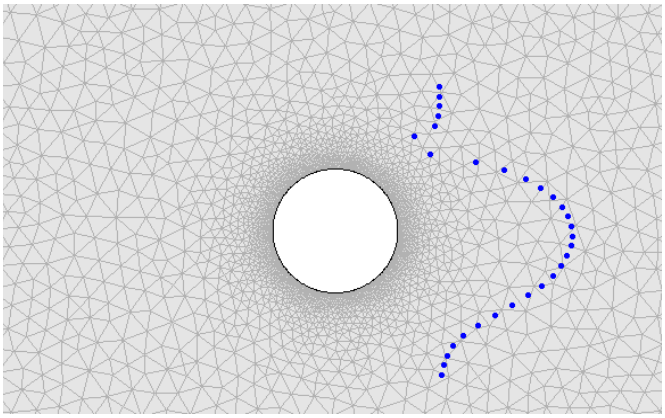

Figure 10: CFD model in COMSOL with simulated tracer particles. Non-Newtonian model with m=0.17, [28].

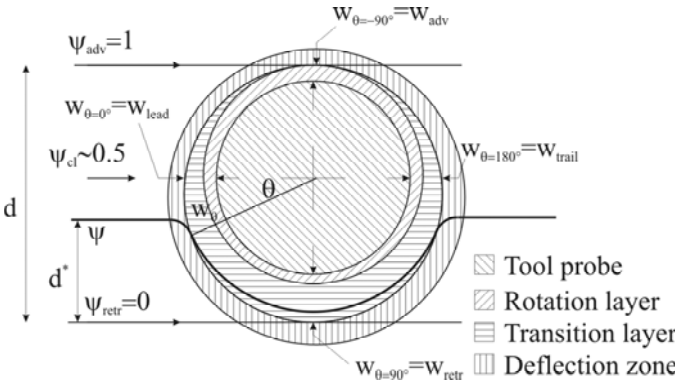

Figure 11: Characteristic zones for the flow around the tool probe: i) the rotation zone. ii) the transition zone and iii) the deflection zone, [28].

Thermal-pseudo-mechanical model

In this paragraph, the author's recently proposed thermal-pseudo-mechanical model [1] is presented. As the name indicates, the model, although being purely thermal from the viewpoint of the classification presented in the present work, still takes some mechanical effects into account without actually solving for any mechanical fields. The main advantage of this is that the obvious simplicity of thermal models is still maintained in the thermal-pseudo-mechanical

model. The basis of the model is to consider the heat generation at a material segment which in general depends on the material flow stress for the given temperature, given strain and given strain rate. The contact stress must be in equilibrium with the material yield shear stress of the underlying material during steady state conditions. This also holds for contact conditions close to sliding, because just for the slightest degree of sticking, i.e. $\delta \sim 0 \ll 1$, see [7] for definition, there will be plastic deformation at the very interface, hence equilibrium between the contact/frictional stress and the material response must prevail. For steady state conditions, this leads to the following relationship

$$\tau_{friction} = \tau_{contact} = \tau_{yield}(T) \tag{4}$$

where $T = T(x, y, z)_{\text{interface}}$ is the non-uniform temperature at the contact interface.

Realizing this, leads to using the material's yield stress to describe the heat generation coming from friction rather than relying on the more classical Coulomb approach which uses the non-uniform pressure distribution and the friction coefficient which in general is a function of the temperature, slip rate, pressure and interface properties (roughness, etc.). Thus, the alternative approach proposed here quantifies the heat generation via the material's yield stress which in general is a function of temperature, strain and strain rates.

However, since it is not the aim to involve a full thermomechanically based solution, only the temperature dependence of the material flow stress is taken into account. This leaves a very important point to be clarified: For which values of ε and $\dot{\varepsilon}$ should the yield stress be chosen? In other words: How should the mechanical history that a material segment experiences during its path through the shear layer be represented? At the present stage, the maximum values of the yield stress resembling a torsion test for a constant strain rate have been chosen.

Summing up, the benefits as compared to classical Coulomb friction are several: a) more data is available for the material's yield response as compared to the friction coefficient μ b) prior knowledge to the pressure distribution is not needed c) the model becomes much more robust towards variations in the input data.

In the thermal pseudo mechanical model, the heat generation contributions from friction and plastic dissipation are now both described as a surface flux and given by

$$\begin{aligned} q_{friction} &= (1-\delta)\omega r \tau_{friction} \\ q_{plastic} &= \delta \omega r \tau_{yield} \end{aligned} \tag{5}$$

Combining these expressions with equation (4) and assuming pure shear yields

$$q_{total} = \omega r \tau_{yield}(T) = \omega r \frac{\sigma_{yield}(T)}{\sqrt{3}} \tag{5}$$

which underlines the fact that the entire heat generation is modelled as a surface flux which is depending on the local temperature. This temperature dependence hence leads to a heat source which is part of the numerical solution itself, making it a non-linear problem to solve. This obviously calls for an iterative procedure. However, it turns out that the price in calculation time is relatively low, i.e. a typical thermal pseudo mechanical model needs approximately twice the calculation time as a normal steady state thermal model of FSW.

It should be underlined that the above described thermal-pseudo-mechanical model will capture the first order effect of the material's mechanical response without making a full thermomechanical model. A very important characteristic about this model is the self-stabilizing effect once temperatures reach the solidus temperature, in which case the heat source "turns itself off". This makes the model effectively more dependent on changes in boundary conditions and welding parameters, rather than e.g. choice of material law. Moreover it should be further underlined that the heat transfer coefficients describing boundary conditions are the only fitting parameters in the model. It is important to emphasize that once these have been found, the effect of welding parameters such as welding velocity and rotational speed can be varied and the model will implicitly capture this in the heat generation and temperature profiles.

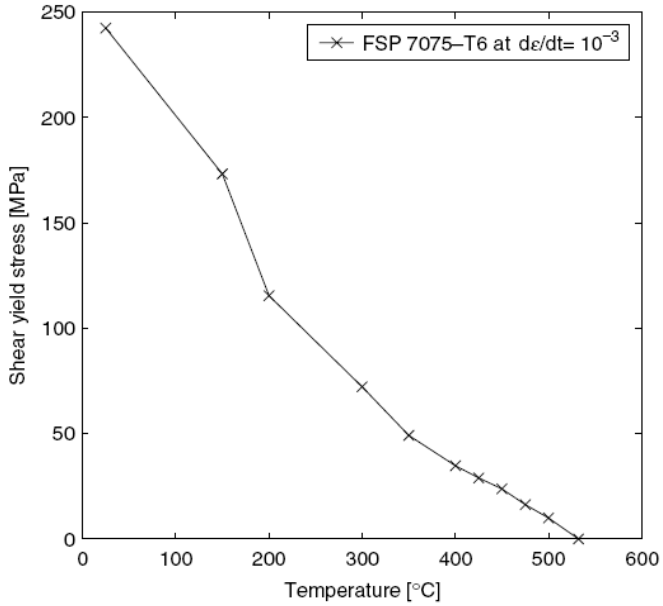

Figure 12: Shear yield stress derived from [29].

The temperature dependent heat source given by equation (5) is implemented in a Eulerian model that, in addition to the workpiece, includes the tool and the backing plate. The thermal model is implemented in Comsol 3.3 and is based on

an experiemental weld of 7075 T6 instrumented with thermocouples. The welding conditions are given in [1] and the thermal properties are taken from [29]. The experimentally found values for the maximal yield stress of friction stir processed 7075 at strain rates of 0.001 1/s are used for the shear yield stress in figure 12. A total of 100.000 degrees of freedom in the model are solved for. A more thorough description of the model can be found in [1].

Figure 13 shows the model results for the local heat generation given by equation (5) evaluated along the intersection between the tool and the joint line. The temperature dependent heat generation denoted by (-) is the result of the thermal-pseudo-mehcanical model and this is compared with the analytically prescribed, linearly dependent heat generation denoted by (--); the latter was evaluated using the same total heat generation as being a result of the former. In the interval under the probe tip, the heat genearation is close to linear since the temperature is nearly constant in this area.

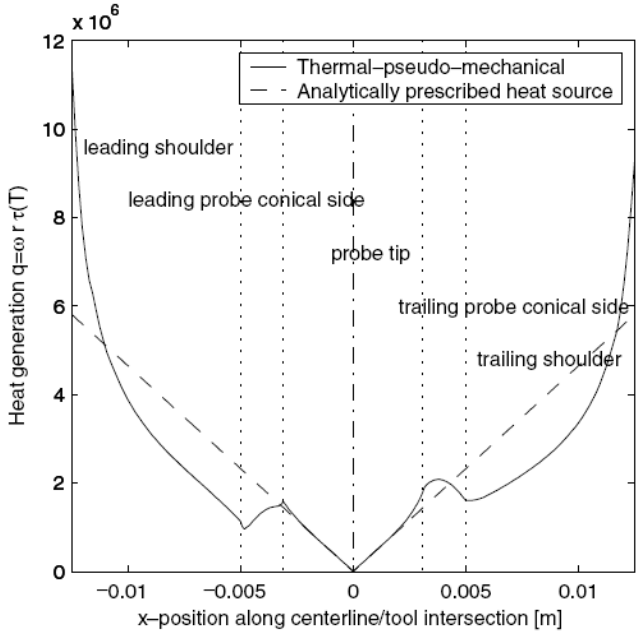

Figure 13: Local heat generation as calculated from eq. (5) evaluated along the intersection between tool and centreline. The total heat generation in the analytical model is prescribed with the value obtained in the thermal-pseudo-mechanical model, [1].

The exponetially increasing heat generation at both the leading and trailing shoulder regions is a combination of the ωr-term and the increase in yield shear stress due to the decrease in temperature for larger radii (here shown as x-values).

The total heat generated at the tool/matrix interface is found to be 1.9 kW (83% from the shoulder, 16% from the conical probe sides and 1% from the probe tip). Moreover, the global thermal efficiency is found to be 88%. Figure 14 shows the corresponding temperatures along the same intersection. It is very obvious that the overestimation of the temperature at the most outer region of the shoulder in the analytical model is avoided by the self-establishing turning off effect of the thermal-pseudo-mehcanical model.

Figure 15 shows a comparison between the experimentally found temperature profiles and the modelling results. The good correleation between the profiels is obtained by adjusting only the heat transfer coefficients/contact resistances. Most important in this context is the coupling between the workpiece and the backing plate.

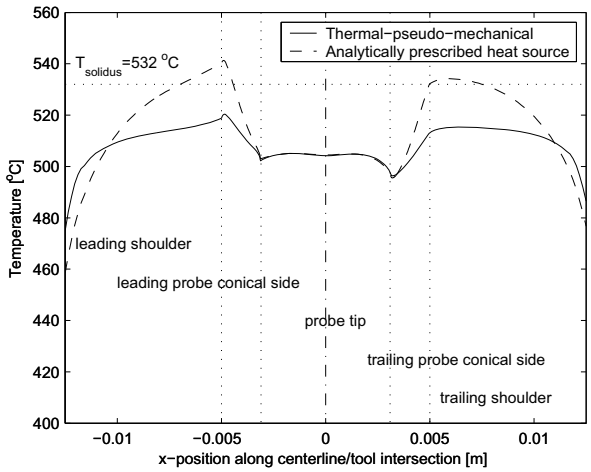

Figure 14: Predicted temperatures along the intersection between tool and centreline, [1].

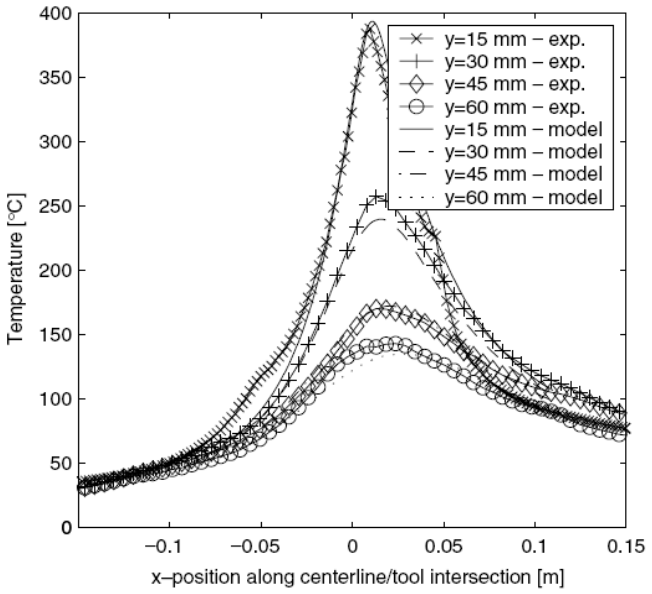

Figure 15: Comparison between the thermal-pseudo-machanical model and experimental results for the far-field temperature profiles at y-values of 15, 30, 45 and 60 mm, [1].

In figure 16 iso-curves for the resulting heat generation are depicted as a function of the welding speed and the rotational speed. Note that for a fixed rotational speed [rpm], increasing the welding speed [mm/s] gives an increase in the heat generation [W]. Similarly for a fixed welding speed, an increase in rotational speed gives an increase in the heat generation. This is also what one would expect.

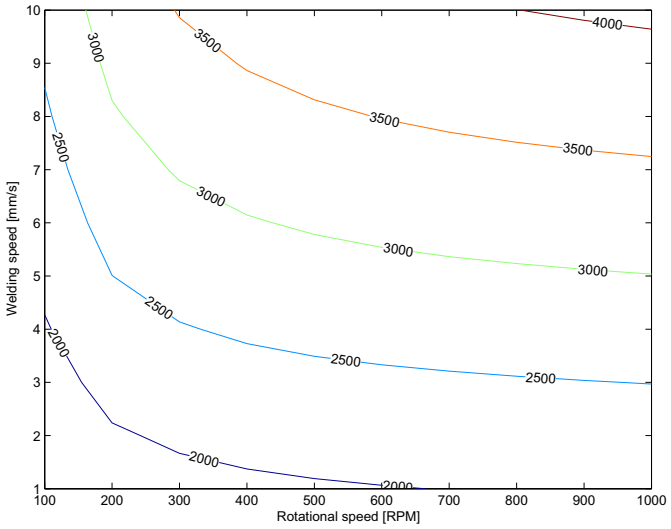

Figure 16: Iso-curves for the resulting heat generation [W] as a function of the welding speed [mm/s] and the rotational speed [rpm], [27].

Figure 17 depicts iso-curves for the maxiamal temperature [ºC] as a function of the rotational speed and welding speed. Here it is noticed that for a fixed rotational speed, increasing the welding speed reduces the maximal temperature and for a fixed welding speed, increasing the rotational speed gives increased maximal temperatures. Note, that the distance between the iso-curves for the maximal temperature becomes increasingly larger when increasing the rotational speed, since the temperature approaches the cut off temperature.

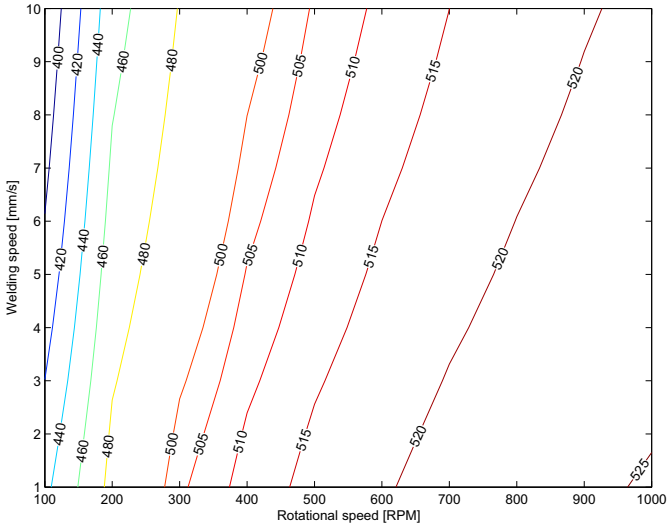

Figure 17: Iso-curves for the resulting maximal temperature [ºC] as a function of the welding speed [mm/s] and the rotational speed [rpm], [27].

The thermal-pseudo-mechanical model presented here is the first attempt to develop a thermal model in which the total heat generation is not an input parameter, but actually a result of the model itself. It should be strongly underlined that the good agreement between the analytically prescribed heat source model and the thermal-pseudo-mechanical model in figure 13 is only achievable when the total heat generation has been found from the latter before being inserted in the former.

Concluding remarks

In the present work, an overview of thermomechanical modelling of FSW has been given. Emphasis has been put on presenting some important basics of the different types of models including thermal models, solid mechanics models and fluid dynamics models. Microstructural models have been excluded from the presentation due to the limited space, however, it should be emphasized that these models are very important for realistic modelling of FSW because of their ability to predict the evolution of the mechanical properties to be used in the thermomechanical models and in particular in models for the in-service behaviour.

Finally, it is fair to say that modelling of FSW now has been established as a field of its own and that we can expect a similar development in this field as in more matured fields of computational welding mechanics (CWM), i.e. a) More combined microstructural-thermomechanical models. b) Integrated process and in-service models. c) More applications on real 3-D structures.

References

1. H. Schmidt and JH. Hattel, *Thermal modelling of friction stir welding, Scripta Materialia.,* 58, 332-337 (2008)
2. M. J. Russel and H. R. Shercliff, *Analytical Modelling of Microstructure Development in Friction Stir Welding*, 1st Int. Symp. On Friction Stir Welding, CA, USA (1999)
3. P. Colegrove, M. Painter, D. Graham and T. Miller, *3-D flow and thermal modelling of the friction stir welding process*, 2nd Int. Symp. On Friction Stir Welding, Sweden (2000)
4. M.Z.H. Khandkar and J.A. Khan, *Thermal model of overlap friction stir welding for Al-alloys, J Materials Processing Manufacture* 10, 91-105 (2001)
5. M. Song and R. Kovacevic, *Thermal modelling of friction stir welding in moving coordinate system and its validation, International Journal of Machine Tool and Manufacturing* 43(6) 605-615 (2003)
6. H. Schmidt, JH. Hattel and J. Wert, *An analytical model for the heat generation in frictions stir welding, Modelling and Simulation in Materials Science and Engineering.,* 12, 143-157 (2004)
7. H. Schmidt and JH. Hattel, *Modelling the heat flow around tool probe in friction stir welding, Science and Technology of Welding and Joining,* 10(2), 176-186 (2005)
8. S. Mandal and K. Williamson, *A thermomechanical hot channel approach for friction stir welding, J Materials Processing Technology*, 190-194 (2006)
9. A. Simar, J. Lecomte-Beckers, T. Pardoen and B. de Meester, *Effect of boundary conditions and heat source*

distribution on temperature distribution in friction stir welding, Science and Technology of Welding and Joining, 170-177 (2006)
10. CC Tutum, H.Schmidt, JH Hattel and MP Bendsøe, *Estimation of the Welding Speed and Heat Input in Friction Stir Welding using Thermal Models and Optimization, Proc. 7th World Congress on Structural and Multidisciplinary Optimization*, Seoul, 2639-2646 (2007)
11. J.K. Raghulapadu, J. Peddieson, G.R. Buchanan and A.C. Nunes, *A rotating plug model of friction stir welding heat transfer, Heat Transfer Engineering*, 29 (3), 321-327, (2008)
12. R.L. Goetz and K.V. Jata, *Modelling friction stir welding of titanium and aluminium alloys*, Proc. Symposium on Friction Stir Welding and Processing, TMS (2001)
13. G. Buffa, J. Hua, R. Shivpuri and L. Fratini, *A continuum based fem model for friction stir welding – model development, Materials Science and Engineering A*, 419, 389-396, (2006)
14. R. K. Uyyury and S.V. Kailas, *Numerical analysis of friction stir welding process, Journal of Materials Engineering and Performance* (2006)
15. A. P. Reynolds, X. Deng, T. Seidel and S. Xu, *Finite element simulation of flow in friction stir welding*, Proc. Joining of Advanced and Specialty Materials, 172-177, MO, USA, (2000)
16. S. Xu and X. Deng, *Two and three-dimensional finite element models for the friction stir welding process*, 4th Int. Symp. On Friction Stir Welding, UT, USA (2003)
17. H. Schmidt and J. Hattel (2005), *A local model for the thermomechanical conditions in friction stir welding, Modelling and Simulation in Materials Science and Engineering*, 13, 77-93, (2005)
18. H. Zhang and Z. Zhang, *Numerical modelling of friction stir welding process by using rate-dependent constitutive model, Journal of Materials Science and Technology*. 23(1), 73-80, (2007)
19. Y.J. Chao and X. Qi, *Heat transfer and thermomechanical analysis of friction stir joining of AA6061-T6 plates*, 1st Int. Symp. On Friction Stir Welding, CA, USA (1999)
20. C.M. Chen and R. Kovacevic, *Finite element modelling of friction stir welding – thermal and thermomechanical analysis, Machine Tools and manufacture*, 43, 1319-1326 (2003)
21. A. Bastier, M.H. Maitournam, K. Dang Van and F. Roger, *Steady state thermomechanical modelling of friction stir welding, Science and Technology of Welding and Joining*, 11(3) 278-288 (2006)
22. C.C. Tutum, H.N.B. Schmidt, J.H. Hattel, *Assessment of benchmark cases for modelling of residual stresses and distortions in friction stir welding*, Proc 7nd Int. Symp. On Friction Stir Welding, Japan (2008)
23. P. A. Colegrove and H.R. Shercliff, *CFD modelling of friction stir welding of thick plate 7449 aluminium alloy, Science and Technology of Welding and Joining*, 11(4), 429-441, (2006)
24. T. Long and A.P. Reynolds, *Parametric studies of friction stir welding by commercial fluid dynamics simulation, Science and Technology of Welding and Joining*, 11(2), 200-208, (2006)
25. R. Nandan, G.G. Roy, T.J. Lienert and T. Debroy, *Three-diemnsional heat and material flow during friction stir welding of mild steel, Acta Materialia*, 55, 883-895, (2007)
26. A.P. Reynolds, *Flow visualization and simulation in FSW, Scripta Materialia*, 58, 338-342, (2008)
27. H. Schmidt and JH Hattel, *Thermal modelling of friction stir welding using a temperature dependent heat source*, Proc 7nd Int. Symp. On Friction Stir Welding, Japan (2008)
28. H.N.B. Schmidt, T.L. Dickerson and J.H. Hattel, *Material flow in butt friction stir welds in AA2024-T3, Acta Materialia*, 54, 1199-1209, (2006)
29. *Metals Handbook*, vol. 2: Properties and Selection: Nonferrous Alloys and Special-Purpose Materials, 10th ed., ASM International, (1990)

ASM International is the society for materials engineers and scientists, a worldwide network dedicated to advancing industry, technology, and applications of metals and materials.

ASM International, Materials Park, Ohio, USA
www.asminternational.org

Publication title	Product code
Trends in Welding Research 2008	**#05254G**

To order products from ASM International:

Online Visit www.asminternational.org/bookstore

Telephone 1-800-336-5152 (US) or 1-440-338-5151 (Outside US)

Fax 1-440-338-4634

Mail Member Service Center, ASM International
9639 Kinsman Rd, Materials Park, Ohio 44073-0002, USA

Email MemberServiceCenter@asminternational.org

In Europe American Technical Publishers Ltd.
27-29 Knowl Piece, Wilbury Way, Hitchin Hertfordshire SG4 0SX, United Kingdom
Telephone: 01462 437933 (account holders), 01462 431525 (credit card)
www.ameritech.co.uk

In Japan Neutrino Inc.
Takahashi Bldg., 44-3 Fuda 1-chome, Chofu-Shi, Tokyo 182 Japan
Telephone: 81 (0) 424 84 5550